Acta Cryst. (1997). B53, 787–794

Structure and Thermal Vibrations of Spermine Phosphate Hexahydrate from Neutron Diffraction Data at 125 K

A. E. COHEN,[a] B. M. CRAVEN[a]* AND W. T. KLOOSTER[b]

[a]*Department of Crystallography, University of Pittsburgh, Pittsburgh, PA 15260, USA, and* [b]*Chemistry Department, Brookhaven National Laboratory, Upton, NY 11973, USA. E-mail: craven@vms.cis.pitt.edu*

(*Received 21 October 1996; accepted 17 April 1997*)

Abstract

Spermine phosphate hexahydrate crystallizes in space group $P2_1/a$ with unit-cell dimensions a = 7.931 (1), b = 23.158 (5), c = 6.856 (2) Å, and β = 113.44 (2)° at 125 K with unit-cell contents $[(C_{10}H_{30}N_4)_2^{4+}(HPO_4)_4^{2-}.12H_2O]$. The packing of spermines and monohydrogen phosphates in this crystal structure has features which may be relevant to the binding of spermine to DNA. Another important structural feature is the presence of channels containing water that is hydrogen bonded as in ice-Ih with disordered protons. The channels occur between sheets of spermine long chains and are also bordered by hydrogen-bonded monohydrogen phosphate chains. The hydrogen-bonding scheme of these water chains proposed on the basis of an earlier X-ray study is now confirmed. Nuclear positions, anisotropic mean-square (m.s.) displacements, an overall scale factor and two extinction parameters (ρ and g) were refined using full-matrix least-squares giving values of $R(F_o^2)$ = 0.09, $Rw(F_o^2)$ = 0.11 and S = 1.02. Thermal vibrational analysis revealed that the backbone of the spermine cation can be described as a single rigid segment with a substantial libration of 27 deg^2 around the spermine molecular long axis.

1. Introduction

Spermine ($C_{10}H_{26}N_4$) is a very water-soluble, strongly basic, aliphatic polyamine widely found in nature. Crystals of spermine phosphate hexahydrate were first observed and described by van Leeuwenhoek (1678). Spermine has a strong affinity for nucleic acids and affects the rate and extent of nucleic acid biosynthesis (for reviews, see Tabor & Tabor, 1976; Morris & Marton, 1981). The crystal structure of spermine phosphate hexahydrate† was first determined by Iitaka & Huse (1965) from X-ray Weissenberg photographic data, but the hydrogen positions were not located. This structure is well suited for a more detailed crystallographic study. It has a centrosymmetric space group, so that there are no ambiguities in phasing the structure factors, and the spermine tetracation lies on a crystallographic inversion center so that the asymmetric unit consists of only half a molecule. Finally, the crystal structure includes water molecules, which display an interesting ice-like configuration. This neutron diffraction study is aimed at providing accurate positional and thermal-vibrational parameters of the atomic nuclei for use in the study of the charge density distribution in the crystal from X-ray data collected at the same low temperature.

† $[(C_{10}H_{30}N_4)_2^{4+}(HPO_4)_4^{2-}.12H_2O]$, sperminium monohydrogen phosphate hexahydrate, is referred to as spermine phosphate hexahydrate in accordance with previously published works and in this text will be subsequently designated as SPH.

2. Experimental

Crystals of SPH were formed by very slow cooling of a solution of spermine phosphate (Sigma Chemical Company) in the presence of phosphoric acid. Differential scanning calorimetry on large single crystals, using a Mettler TA4000 system, showed no crystal phase transitions as the temperature was lowered from room temperature down to 115 K. The crystal used for neutron diffraction data collection was elongated along the c axis, with well developed (010) faces. The crystal dimensions were approximately 3.4 × 0.75 × 1.5 mm and the crystal mass was 4 mg. The crystal was glued to a hollow aluminum pin and placed into an aluminum can, which was then sealed and filled with helium. The crystal was then cooled to 125 K using a closed-cycle refrigerator.† Neutron data were collected using the four-circle diffractometer at the H6S station of the High Flux Beam Reactor at Brookhaven National Laboratory. The 220 reflection from a germanium crystal was used to obtain a monochromatic neutron beam with wavelength 1.16395 (10) Å. The unit-cell dimensions, a = 7.931 (1), b = 23.158 (5), c = 6.856 (2) Å, and β = 113.44 (2)° at 125.0 (5) K with two formula units in the unit cell, were determined through a least-squares fit of setting angles for 32 reflections in the range $50 < 2\theta < 61°$. The integrated intensity data were obtained by means of $\omega/2\theta$ step scans for the quadrant of reciprocal space having indices ranging from –10 to 10 in h, 0 to 33 in k and 0 to 9 in l. The data collection was divided into two

† DISPLEX model CS-202, APD Cryogenics, Inc.

shells with $\sin\theta/\lambda$ limiting values of 0.43 and 0.68 Å^{-1}. Scan widths were constant in the first shell ($\Delta 2\theta$ = 2.4°), but variable for the second shell [$\Delta 2\theta$ = 1.097° + 5.935tan(θ)]. Two standard reference reflections (412 and $\bar{6}92$) measured at intervals of 50 reflections showed no significant variation of intensity with time. A total of 3378 reflections were measured. Data processing was carried out by a series of computer programs developed by Blessing (1989), which were all modified for use with neutron diffraction data. Integrated intensities and variances were derived from the scan profiles. Each scan profile was examined (Spackman, 1987) and, if necessary, the scan limits were shifted to exclude contributions to the background by neighboring reflections and aluminum powder lines. Peak overlap was very severe for 135 reflections, which were therefore omitted. An analytical correction for neutron absorption with μ = 0.345 mm^{-1} was made (Templeton & Templeton, 1973). Transmission factors ranged between 0.60 and 0.76, with an average factor of 0.72. Symmetry-related reflections were found to be in good agreement, $R(F_o^2)_{\rm int}$ = 0.015 [$R(F^2)_{\rm int} = \Sigma_i|<F_o^2> - F_o^2|/\Sigma<F_o^2>$], and were averaged to give 2873 independent observations. Of these reflections, 2446 had intensities greater than 2σ and 2 reflections were in the range between -2σ and -5σ.

2.1. *Structure refinement*

Using initial non-H-atom positions from the X-ray study of Iitaka & Huse (1965) the crystal structure was first refined by differential Fourier synthesis (McMullan, 1976). A difference-Fourier map revealed the nondisordered hydrogen positions. The disordered hydrogen positions were located from examination of a Fourier map (Shiono, 1972). All reflections were subsequently included in a full-matrix least-squares refinement (Craven & Weber, 1987), in which extinction is treated according to Sabine (1992*a*). The residual $\Sigma w\Delta^2$ was minimized with $w = \sigma^{-2}(F_o^2)$ and $\Delta = F_o^2 - F_c^2$. A total of 354 variables were refined, including nuclear positions, anisotropic m.s. displacements, an overall scale factor and two extinction parameters (ρ and g). The 003 reflection was most affected by extinction (y = 0.58, where $y = I_o^{\rm ext}/I_k$). Coherent scattering lengths were assumed to be 6.648, 9.360, 5.803 and –3.741 fm for carbon, nitrogen, oxygen and hydrogen, respectively (Koester, 1977). The refinement was completed with $R(F_o^2)$ = 0.09, $wR(F_o^2)$ = 0.11 and S = 1.02 with 2519 degrees of freedom.† Final values of the nuclear parameters are listed in Table 1. The extinction parameters, obtained for a model with crystal mosaic blocks scattering without correlations in phases (Sabine, 1992*b*), give a Gaussian distribution of mosaic blocks with a standard deviation of η = 0.58 (3)", where $\eta = 1/(2\pi^{1/2}g)$ and a block size of 361 (10) µm.

† $R(F^2) = (\Sigma|\Delta|)/\Sigma F_o^2$, $wR(F^2) = [(\Sigma w\Delta^2)/(\Sigma wF_o^2)^2]^{1/2}$, $S = [(\Sigma w\Delta^2)/(m-n)]^{1/2}$, where $\Delta = |F_o|^2 - |F_c|^2$.

Table 1. *Fractional atomic coordinates for SPH*

$U_{\rm eq} = (1/3)\Sigma_i\Sigma_j U^{ij} a_i^* a_j^* \mathbf{a}_i.\mathbf{a}_j$.

	x	y	z
N1	0.7107 (1)	0.09375 (6)	−0.0027 (3)
N2	0.1646 (2)	0.21083 (6)	−0.0627 (2)
C1	0.9656 (2)	0.03124 (8)	−0.0094 (3)
C2	0.7785 (3)	0.03342 (8)	0.0018 (3)
C3	0.5206 (2)	0.09474 (8)	−0.0117 (3)
C4	0.4468 (3)	0.15576 (8)	−0.0264 (3)
C5	0.2535 (2)	0.15316 (8)	−0.0302 (3)
W1	0.1176 (4)	0.0467 (1)	0.5460 (4)
W2	0.4170 (3)	0.0529 (1)	0.4380 (4)
W3	0.6652 (3)	0.1465 (1)	0.5978 (4)
P	−0.0047 (3)	0.19654 (9)	0.3684 (4)
O1	−0.0735 (3)	0.21066 (9)	0.1328 (3)
O2	−0.0233 (3)	0.24703 (9)	0.5021 (4)
O3	−0.0980 (3)	0.14162 (9)	0.4011 (3)
O4	0.2072 (3)	0.18018 (9)	0.4534 (4)
H1N1	0.7135 (5)	0.1164 (2)	−0.1343 (7)
H2N1	0.7945 (5)	0.1155 (2)	0.1370 (7)
H1C1	1.0635 (6)	0.0575 (2)	0.1171 (7)
H2C1	0.9571 (6)	0.0495 (2)	−0.1614 (7)
H1C2	0.7834 (6)	0.0134 (2)	0.1490 (7)
H2C2	0.6762 (5)	0.0106 (2)	−0.1341 (7)
H1C3	0.5226 (6)	0.0731 (2)	0.1309 (8)
H2C3	0.4335 (6)	0.0693 (2)	−0.1505 (7)
H1C4	0.4419 (6)	0.1769 (2)	−0.1720 (7)
H2C4	0.5367 (6)	0.1812 (2)	0.1124 (8)
H1C5	0.2561 (6)	0.1363 (2)	0.1211 (7)
H2C5	0.1665 (6)	0.1246 (2)	−0.1583 (8)
H1N2	0.0638 (5)	0.2111 (2)	0.0009 (7)
H2N2	0.1025 (6)	0.2222 (2)	−0.2235 (6)
H3N2	0.2651 (2)	0.2427 (4)	0.0192 (6)
H1*W*1†	0.2170 (20)	0.0500 (4)	0.5026 (16)
H2*W*1	0.0431 (6)	0.0822 (2)	0.4979 (7)
H3*W*1†	0.0361 (13)	0.0161 (4)	0.5162 (15)
H1*W*2	0.4932 (7)	0.0870 (2)	0.4877 (8)
H2*W*2	0.3110 (4)	0.0553 (5)	0.4731 (17)
H3*W*2†	0.4847 (14)	0.0184 (5)	0.4805 (17)
H1*W*3†	0.7557 (6)	0.1460 (2)	0.5333 (7)
H2*W*3	0.6056 (6)	0.1844 (2)	0.5632 (7)
HO4	0.2956 (5)	0.2119 (2)	0.4598 (6)

† Disordered atoms with occupancy 0.5.

2.2. *Thermal vibrational analysis*

In Figs. 1 and 2 it can be seen that the 50% probability ellipsoids enclosing the hydrogen nuclei of the spermine tetracation and monohydrogen phosphate are consistently larger than those for the C, N, O and P nuclei. The considerably greater size of the H-ellipsoids suggests that for the hydrogen nuclei, intramolecular nonrigid C—H, N—H and O—H thermal vibrations are appreciable. The difference in m.s. amplitudes of nuclear displacement along the interatomic vector for nuclei A and B was determined from $U_{\rm obs}^{ij}$, $\Delta(A,B) = < u_B^2 >< u_A^2 >$. A significant nonzero value for $\Delta(A,B)$ indicates that nuclei A and B are vibrating nonrigidly (Hirshfeld, 1976). The Hirshfeld test (Hirshfeld, 1976) indicates nonrigidity for nuclear vibrations in monohydrogen phosphate along interatom vectors involving the H atom. Along the HO4—O4 bond, Δ = 0.0065 (26) Å^2 with a significance level of 2.5σ. For the heavier atoms, values of Δ are small. The largest of these, Δ = 0.0025 (14) Å^2, is along the P—O3 bond direction. Also, for the non-H backbone of the spermine cation values of $\Delta(A,B)$

are very small and insignificant; for example, Δ = 0.0002 (13) Å^2 for N2···C5′ and the largest difference is Δ = 0.0027 (16) Å^2 for C4···C5. In contrast, nonrigidity is strongly indicated for most covalent bonds involving H atoms (Table 2). For instance, along the C4—H2C4 bond, Δ = 0.0077 (22) Å^2 and along the N1—H2N1 bond, Δ = 0.0067 (19) Å^2.

Analysis of nuclear anisotropic m.s. displacements for the hydrogen nuclei of the spermine cation (Table 1) began by using the simple rigid-body model (Schomaker & Trueblood, 1968) for the backbone (C and N) nuclear vibrations. Because the cation has a crystallographic center of symmetry, only the rigid body **T** and **L** tensors need be considered. The residual, $\Sigma w(U^{ij}_{obs} - U^{ij}_{calc})^2$ with $w = 1/\sigma^2(U_{eq})$, was minimized by least-squares (He & Craven, 1993), giving an agreement with wR = 0.088 and S = 1.23 ($wR = [(\Sigma w\Delta^2)/(\Sigma w U^{ij}_{obs})^2)]^{1/2}$, where $\Delta = U^{ij}_{obs} - U^{ij}_{calc}$) and the sum includes all six U^{ij} components for all atomic nuclei; $S = [\Sigma w\Delta^2/(m - n)]^{1/2}$ with $(m - n)$ = 72). In the least-squares fit the T_{11} (translation normal to the plane of the C and N nuclei) and L_{33} tensor components (libration around the molecular long axis) are highly correlated (94%), because the atomic nuclei of the molecular backbone lie nearly on one of two parallel straight lines (Johnson, 1970). In order to overcome this problem anisotropic m.s. displacement parameters of the methylene H nuclei were added to the rigid-body calculation. Before a rigid-body model can be fitted to the observed anisotropic thermal vibrations of hydrogen atomic nuclei, it is necessary to correct for the internal molecular motion of the hydrogen nuclei (Johnson, 1970). Values of the internal m.s. displacements of methylene H nuclei, U^{ij}_{int}, were taken from a previous neutron diffraction study of piperazinium hexanoate (Luo, Ruble, Craven & McMullan, 1996). The average principal values of the internal m.s. displacements of methylene H nuclei used were U_1 = 5×10^{-4}, U_2 = 174×10^{-4} and U_3 = 174×10^{-4} Å^2, where U_1 corresponds to bond stretching along the C—H bond, U_2 is a displacement in the H—C—H plane and U_3 is a displacement normal to the H—C—H plane. The residuals, assumed to represent the external component of the anisotropic m.s. displacements for the methylene H nuclei, U^{ij}_{ext}, and the observed m.s. displacements, U^{ij}_{obs}, for the framework nuclei (C and N) were all included in a subsequent least-squares fit to the rigid-body model. A good fit was obtained with wR = 0.114 and S = 1.162, where $(m - n)$ = 192. The correlation between T_{11} and L_{33} became insignificant and a substantial libration [L_{33} = 27 (1) deg^2] around the molecular long axis was obtained. The Hirshfeld test (Hirshfeld, 1976) does not rule out the presence of internal torsional vibrations of the chain since these involve displacements close to the normal of the planar spermine backbone. Such torsional modes were found for the hydrocarbon chain in suberic acid (Gao, Weber, Craven & McMullan, 1994). Although models of this type were tested, none gave improved agreement over the simple rigid-body model for the spermine chain. The value of L_{33} is certainly an overestimate because it includes the effect of nonrigid modes.

The rigid-body parameters listed in Table 2 were then used in order to calculate the rigid-body contribution to the m.s. displacements of each amine H nucleus. This value was subtracted from U^{ij}_{obs} for each ammonium H nucleus to give U^{ij}_{int}, the intramolecular component of the m.s. displacements. These residual values were transformed to a local Cartesian axial system with U^{11}_{int} along the N—H bond, U^{22}_{int} in the plane of the NH_2 group and normal to the N—H bond, and U^{33}_{int} along the normal to the plane of the NH_2 group. Thus, U^{11}_{int} corresponds to bond stretching along the N—H bond, U^{22}_{int} is a displacement in the H—N—H plane and U^{33}_{int} is a displacement normal to the H—N—H plane.† Table 2 shows these values of U^{ij}_{int} with respect to the local Cartesian axial system described above, as well as the principal values of these tensors in the local axial system.

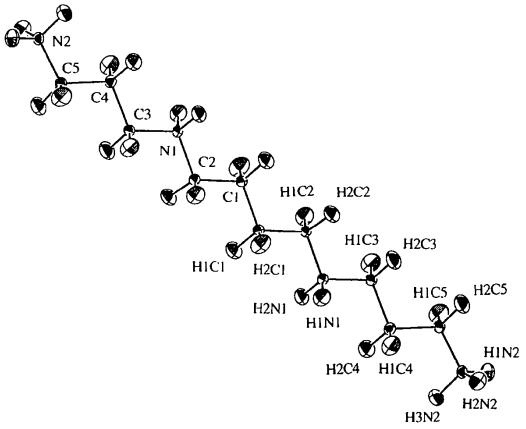

Fig. 1. Thermal ellipsoid plot for the spermine tetracation at 50% probability for enclosing the atomic nuclei (Johnson, 1976).

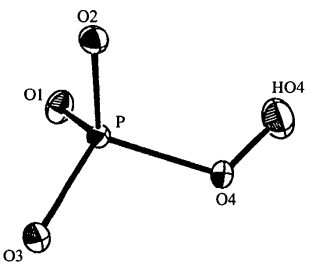

Fig. 2. Thermal ellipsoid plot for the monohydrogen phosphate ion at 50% probability for enclosing the atomic nuclei (Johnson, 1976).

† For NH_3, U^{11}_{int} corresponds to bond stretching along the N—H bond, U^{22}_{int} is an umbrella-type vibration in the C—N—H plane and U^{33}_{int} is an internal torsional libration about the C—N bond.

Table 2. *Analysis of the nuclear m.s. displacement parameters*

(*a*) Molecular framework vibrations

Both the spermine and the monohydrogen phosphate ions are each treated as having one rigid segment. The rigid-body **T**, **L** and **S** tensor components (Schomaker & Trueblood, 1968) are with respect to the principal axes of the moments of inertia with the origin at the center of mass. The axes I_1, I_2 and I_3 are in the order of decreasing moment of inertia; such that for the spermine cation, I_1 is normal to the best plane of the framework (C and N) nuclei and I_3 is along the molecular long axis. The first column is for the rigid-body calculation for the spermine cation which includes U^{ij}_{ext}, calculated external m.s. displacement parameters of the methylene H atoms, as well as U^{ij}_{obs} of the molecular framework (C and N) atoms. The second column is for the monohydrogen phosphate anion with the H atom omitted from the rigid-body calculation.

	Spermine cation	Monohydrogen phosphate anion
Translational tensor, **T** (Å^2 × 10^4)		
T_{11}	141 (3)	95 (7)
T_{22}	107 (3)	115 (7)
T_{33}	100 (2)	87 (7)
T_{12}	−9 (3)	−9 (6)
T_{13}	−3 (2)	−13 (6)
T_{23}	15 (2)	9 (5)
Principal values		
	145	96
	115	123
	88	77
Librational tensor, **L** (deg^2)		
L_{11}	0 (1)	8 (3)
L_{22}	0 (1)	7 (3)
L_{33}	27 (1)	6 (3)
L_{12}	0 (1)	2 (2)
L_{13}	0 (1)	2 (2)
L_{23}	0 (1)	1 (2)
Principal values		
	0	11
	0	6
	27.2	5
Cross Tensor, **S** (Ådeg × 10^2)†		
S_{11}	0	5 (5)
S_{12}	0	−2 (2)
S_{13}	0	2 (2)
S_{21}	0	1 (2)
S_{22}	0	−4 (5)
S_{23}	0	1 (2)
S_{31}	0	1 (2)
S_{32}	0	5 (2)
S_{33}	0	−10
Goodness of fit	1.16	0.96
wR(*U*)	0.011	0.053

(*b*) M.s. amplitudes of internal vibrations (Å^2 × 10^{-4})

Columns are as follows: $\Delta_{A-B} = < u_B^2 > - < u_A^2 >$, which is the difference in m.s. amplitudes of nuclear displacement along the interatom vector for nuclei *A* and *B* as determined from U^{ij}_{obs} (Hirshfeld, 1976). U^{ij} are the components of the difference tensor $U^{ij}_{int} = U^{ij}_{obs} - U^{ij}_{ext}$ referred to the local Cartesian axial system for each H nucleus. The local axes are defined in terms of the internuclear vectors **u** and **v**. For example, for the H1N1 atom of the spermine cation, **u** is along the N1—H1N1 bond and **v** is along the N1—H2N1 bond. The local *x* axis is along the N1—H1N1 bond; the local *y* axis is normal to the N1—H1N1 bond and within the NH_2 plane; and the local *z* axis is along **u** × **v** which is normal to the plane of the NH_2 group. Thus, U^{11} is an internal m.s. displacement along the N1—H1N1 bond, U^{22} is a displacement in the H2N1—N1—H1N1 plane and U^{33} is a displacement normal to the H2N1—N1—H1N1 plane. For the HO4 H atom the first local *x* axis is along the O—H bond; the local *y* axis is in the P—O—H plane normal to the O—H bond and the local *z* axis is normal to the P—O—H plane. For the second local axial system for the HO4 atom the *x* axis is along the HO4···O2 hydrogen bond, the *y* axis is normal to the HO4···O2 hydrogen bond and within the O2···HO4—O4 plane, and the *z* axis is normal to the O2···HO4—O4 plane. U_1, U_2 and U_3 are the principal values of U^{ij}_{int}.

Table 2 (*cont.*)

	Δ_{A-B}	U^{11}	U^{22}	U^{33}	U^{12}	U^{13}	U^{23}	U_1	U_2	U_3
H1N1	49 (30)	41	95	119	11	7	−7	38	96	121
H2N1	67 (19)	60	51	112	−19	7	3	75	35	113
H1N2	39 (34)	25	148	152	−37	−20	−5	12	159	154
H2N2	65 (20)	67	131	53	−75	26	18	87	135	28
H3N2	56 (19)	48	127	90	−29	12	78	66	191	8
HO4	65 (26)	57	109	13	9	3	20	56	114	9
HO4		56	99	24	1	4	36			

† For the cation, the constraint $S_{ij} = 0$ was imposed since the spermine cation lies on a crystallographic inversion center.

For the H1N1 nucleus the principal values are similar to the diagonal components of the U^{ij}_{int} tensor and the off-diagonal components are relatively small. Thus, the principal values are for vibrations in directions close to those of the local axial system. However, for the other ammonium hydrogens (H2N1 and the terminal H1N2, H2N2 and H3N2) this is not the case and the off-diagonal terms of the U^{ij}_{int} tensors are significant. The vibrations of these H nuclei seem to be influenced by the effects of intermolecular N—H···O hydrogen bonding.

With the hydrogen nucleus omitted, the monohydrogen phosphate anion was analyzed in terms of a simple rigid-body model (Schomaker & Trueblood, 1968). The U^{ij}_{obs} values were fitted to a rigid-body model by least-squares (He & Craven, 1993), resulting in a good fit with $wR = 0.053$ and $S = 0.96$, where $(m - n) = 10$. The rigid-body contribution to the m.s. displacements of the HO4 atomic nucleus, U^{ij}_{ext}, was then calculated using the parameters listed in Table 2. The differences $(U^{ij}_{obs} - U^{ij}_{ext}$, are assumed to represent U^{ij}_{int}, the intramolecular m.s. displacements. Table 2 also lists these residuals, which have been transformed to a local atomic axial system with U^{11}_{int} along the OH bond, U^{22}_{int} in the P—O—H plane normal to the O—H bond and U^{33}_{int} normal to the P—O—H plane. For the HO4 atom the principal values are for vibrations in directions close to those of the local axial system, but the value of U^{33}_{int}, 13×10^{-4} Å^2, is smaller than expected. The nonrigid m.s. displacements of HO4 seem to be influenced by the effects of intermolecular O—H···O hydrogen bonding. The HO4 atom is involved in a hydrogen bond with O2 of a neighboring monohydrogen phosphate anion (Table 5). Table 2 lists U^{ij}_{int} for the HO4 atoms transformed into a second local axial system. In this axial system U^{11}_{int} is along the HO4···O2 hydrogen bond, U^{22}_{int} is normal the the HO4···O2 hydrogen bond and within the O2···HO4—O4 plane, and U^{33}_{int} is normal to the O2···HO4—O4 plane. In this second system the value of U^{33}_{int} is increased to 24×10^{-4} Å^2.

3. Discussion

3.1. *Molecular geometry and crystal packing*

The bond lengths and angles of the monohydrogen phosphate ion and water molecules, as well as the bond

lengths and angles of the spermine cation, are listed in Table 3.† Thermal vibrational corrections of bond lengths of the C and N atoms are small and within the e.s.d.'s of the uncorrected values. The average values for the C—C and C—N bond lengths corrected for thermal libration are 1.526 (8) and 1.489 (5) Å. The C—C and C—N bond lengths are all in close agreement. The largest difference of a bond length from the average value is 0.01 Å for C1—C1′. Thermal vibrational corrections for the C—H and N—H bond lengths have not been made, since it is expected that the corrections for harmonic and anharmonic motion are likely to be almost equal and opposite (Ibers 1959; Craven & Swaminathan, 1984), and with an uncertainty comparable to the net correction. The average C—H and N—H bond lengths are 1.098 (4) and 1.054 (8) Å. The length of the P—O4 bond, 1.591 Å, is significantly longer than the other P—O bonds, as is to be expected. The monohydrogen phosphate ion has O—P—O bond angles in the range 104.5 (2)–113.1 (2)° (Table 3) with the smaller angles involving the longer P—O4 bond. The average O*w*—H bond length is 0.96 (2) Å.

The spermine tetracation, $[NH_3(CH_2)_3NH_2(CH_2)_4NH_2(CH_2)_3NH_3]^{4+}$, as shown in Fig. 1, has an extended all *trans* conformation. It has a crystallographic inversion center and the non-H atoms of the spermine chain are almost coplanar, with the largest deviation out of the best least-squares plane being 0.11 Å. The torsion angles of the spermine tetracation are listed in Table 4. In the crystal structure of spermine pyrophosphate hexahydrate (Labadi, Sillanpää & Lönnberg, 1992) the spermine cation also adopts an extended conformation with the largest deviation from a planar arrangement at the C4—C3—N1—C2 segment. The torsion angle about C3—N1 is 171.4 (2)°. The spermine tetracation chain is almost fully extended in the crystal structure of spermine tetranitrate (Jaskólski, 1987), with all bonds *trans* except the *gauche* terminal N2—C5—C4—C3 torsion angle of –65.0 (4)°. In contrast, in the crystal structure of spermine tetrahydrochloride (Giglio, Liquori, Puliti & Ripamonti, 1966) the spermine tetracation is bent with *gauche* turns at the C2—N1 bonds with a C1—C2—N1—C3 torsion angle of 66.0° such that the non-H atoms of the chain consist of three approximately planar groups. In all of these crystal structures the spermine tetracation has a crystallographic center of symmetry. However, there seems to be some conformational flexibility. It is also interesting to consider the spermidine phosphate trihydrate crystal structure (Huse & Iitaka, 1969), in which there are two crystallographically independent spermidine trications $[NH_3^+(CH_2)_3NH_2^+(CH_2)_4NH_3^+]$. Both these trications exist in a normal extended configuration, with one being almost coplanar, while the second is slightly rippled, with the largest deviations out of the best least-squares plane being approximately 0.2 Å.

The crystal structure of SPH is made up of two types of alternating sheets. The first consists of spermine tetracations. Monohydrogen phosphate ions and water molecules link by hydrogen bonding to form the second type of sheet. The two types of sheets stack parallel to the (001) plane and are held together by N—H···O hydrogen bonds.

The structure of the tetracation sheet is shown in Fig. 3. The spermine chains are tilted ~57° from the *b* axis and adjacent chains related by the *a* glide are oppositely inclined. The shortest chain-to-chain distance.

† Lists of atomic coordinates, anisotropic displacement parameters and structure factors have been deposited with the IUCr (Reference: BK0042). Copies may be obtained through The Managing Editor, International Union of Crystallography, 5 Abbey Square, Chester CH1 2HU, England.

Table 3. *Selected geometric parameters (Å, °)*

Spermine cation			
N1—C2	1.493 (2)	N2—H3N2	1.067 (5)
N1—C3	1.485 (2)	C1—H1C1	1.092 (5)
N2—C5	1.485 (2)	C1—H2C1	1.101 (5)
C1—C1′	1.533 (3)	C2—H1C2	1.096 (5)
C1—C2	1.518 (3)	C2—H2C2	1.097 (5)
C3—C4	1.518 (3)	C3—H1C3	1.093 (5)
C4—C5	1.525 (3)	C3—H2C3	1.098 (5)
N1—H1N1	1.051 (5)	C4—H1C4	1.099 (5)
N1—H2N1	1.054 (5)	C4—H2C4	1.106 (5)
N2—H1N2	1.053 (5)	C5—H1C5	1.100 (5)
N2—H2N2	1.047 (5)	C5—H2C5	1.096 (5)
Monohydrogen phosphate			
P—O1	1.521 (3)	P—O4	1.591 (3)
P—O2	1.528 (3)	O4—HO4	1.004 (5)
P—O3	1.532 (3)		
Water molecules			
*W*1—H2*W*1	0.990 (6)	*W*2—H2*W*2	0.964 (12)
*W*1—H1*W*1	0.949 (13)	*W*2—H3*W*2	0.943 (11)
*W*1—H3*W*1	0.925 (11)	*W*3—H1*W*3	0.981 (5)
*W*2—H1*W*2	0.968 (6)	*W*3—H2*W*3	0.979 (5)
Spermine cation			
C2—N1—C3	111.5 (1)	H2N2—N2—H3N2	108.7 (4)
N2—C5—C4	112.4 (2)	H1N1—N1—H2N1	108.7 (4)
N1—C2—C1	112.4 (2)	H1C1—C1—H2C2	107.2 (4)
N1—C3—C4	112.1 (2)	H1C2—C2—H2C2	108.9 (4)
C1′—C1—C2	110.4 (2)	H1C3—C3—H2C3	108.1 (4)
C3—C4—C5	108.8 (2)	H1C4—C4—H2C4	108.8 (4)
H1N2—N2—H2N2	108.5 (4)	H1C5—C5—H2C5	108.2 (4)
H1N2—N2—H3N2	107.9 (4)		
Monohydrogen phosphate			
O1—P—O2	113.1 (2)	O2—P—O4	107.6 (2)
O1—P—O3	110.1 (2)	O3—P—O4	104.5 (2)
O2—P—O3	112.4 (4)	HO4—O4—P	117.4 (3)
O1—P—O4	108.7 (2)		
Water molecules			
H1*W*1—*W*1—H2*W*1	106.8 (8)	H1*W*2—*W*2—H3*W*2	112.5 (8)
H1*W*1—*W*1—H3*W*1	125.9 (10)	H2*W*2—*W*2—H3*W*2	114.7 (10)
H2*W*1—*W*1—H3*W*1	106.8 (8)	H1*W*3—*W*3—H2*W*3	105.7 (5)
H1*W*2—*W*2—H2*W*2	110.5 (8)		

Table 4. *Torsion angles (°) of the spermine backbone C and N atoms*

Sign is positive if, viewed from second to third atom, clockwise motion superimposes first on fourth atom.

C3—N1—C2—C1	174.8 (2)	C1′—C1—C2—N1	176.6 (2)
C2—N1—C3—C4	−177.5 (2)	N1—C3—C4—C5	−178.8 (2)
C2—C—C1′—C2′	180.0	C3—C4—C5—N2	−175.2 (2)

DOCKET ALARM

Explore Litigation Insights

Docket Alarm provides insights to develop a more informed litigation strategy and the peace of mind of knowing you're on top of things.

Real-Time Litigation Alerts

Keep your litigation team up-to-date with **real-time alerts** and advanced team management tools built for the enterprise, all while greatly reducing PACER spend.

Our comprehensive service means we can handle Federal, State, and Administrative courts across the country.

Advanced Docket Research

With over 230 million records, Docket Alarm's cloud-native docket research platform finds what other services can't. Coverage includes Federal, State, plus PTAB, TTAB, ITC and NLRB decisions, all in one place.

Identify arguments that have been successful in the past with full text, pinpoint searching. Link to case law cited within any court document via Fastcase.

Analytics At Your Fingertips

Learn what happened the last time a particular judge, opposing counsel or company faced cases similar to yours.

Advanced out-of-the-box PTAB and TTAB analytics are always at your fingertips.

API

Docket Alarm offers a powerful API (application programming interface) to developers that want to integrate case filings into their apps.

LAW FIRMS
Build custom dashboards for your attorneys and clients with live data direct from the court.

Automate many repetitive legal tasks like conflict checks, document management, and marketing.

FINANCIAL INSTITUTIONS
Litigation and bankruptcy checks for companies and debtors.

E-DISCOVERY AND LEGAL VENDORS
Sync your system to PACER to automate legal marketing.